

## COMMUNICATION

## Facile Formation of Giant Elastin-like Polypeptide Vesicles as Synthetic Cells

Received 00th January 20xx,  
Accepted 00th January 20xx

DOI: 10.1039/x0xx00000x

Bineet Sharma<sup>a</sup>, Yutao Ma<sup>b</sup>, Harrison L Hiraki<sup>c</sup>, Brendon M Baker<sup>c,d</sup>, Andrew L Ferguson<sup>b</sup> and Allen P Liu<sup>\*a,c,e,f</sup>

**We demonstrate the facile and robust generation of giant peptide vesicles by using emulsion transfer method. These robust vesicles can sustain chemical and physical stresses. Peptide vesicles can host cell-free expression reactions by encapsulating essential ingredients. We show incorporation of another cell-free expressed elastin-like polypeptides into existing peptide vesicle's membrane.**

Synthetic cells are cell-like compartments in the form of membrane vesicles that recreate some aspects of cellular biochemistry.<sup>1,2</sup> A synthetic cell provides a framework where internally encapsulated materials are protected from the external aqueous environment with minimum leakage. Ideally, the protecting boundary should be mechanically strong and semi-permeable for nutrients and gaseous exchange. Various amphiphilic molecules have been employed to create a robust cell-like system, including phospholipids,<sup>3,4</sup> fatty acids,<sup>5</sup> polymers,<sup>6</sup> double emulsion,<sup>7,8</sup> and a hybrid of protein-polymer<sup>9</sup> or lipid-polymer.<sup>10</sup> Phospholipid bilayer vesicles hold the most resemblance to natural cell membrane and have also been employed as drug delivery vehicles.<sup>11</sup> The application of these materials in applied synthetic cell research is impacted by their high susceptibility towards physical stresses (osmotic shock) and mechanical deformation and chemical stress like oxidation in response to pH change and surfactants. Polymersomes with improved mechanical strength have been introduced,<sup>12,13</sup> and

the use of synthetic polymer in building synthetic cells continues to grow.<sup>14</sup>

Recently, a genetically encoded elastin-like polypeptide (ELP) was introduced in a synthetic cell model and its cell-free synthesis was demonstrated.<sup>15,16</sup> ELP has a basic structure of a repeating pentapeptide entity Val-Pro-Gly-X-Gly, where the guest residue X can be any natural amino acid except proline. ELPs exhibit a reversible lower critical solution temperature (LCST) behavior and phase transition, above a temperature ( $T_t$ ). ELPs remain soluble when the temperature is lowered below  $T_t$ .<sup>17</sup> Based on this, ELPs can be purified by an inverse transition cycling (ITC) method.<sup>18</sup> Although ELPs have been shown to form ~50 nm unilamellar vesicles,<sup>19</sup> there are few examples of generating cell-sized ELP vesicles. This is in part due to the propensity for ELPs to form an array of micellar structures. Here, we hypothesized that amphiphilic ELPs may be able to form bilayer vesicles when presented with a template.

We start with an amphiphilic ELP (denoted as S48I48) that comprises 48 repeats of pentapeptide (VPGXG) blocks of serine and isoleucine as the guest residue for the hydrophilic and hydrophobic domains, respectively (Fig. 1A). S48I48 displays partial transition at 27°C due to self-assembly of isoleucine blocks and bulk phase transition at 75°C due to aggregation of serine blocks.<sup>20</sup> S48I48 was expressed and purified from *E. coli* by three cycles of ITC at 37°C and the purity of a lyophilized ELP was confirmed by SDS-PAGE (Fig. S1, ESI).

We next demonstrate a robust method for generating giant ELP vesicles as synthetic cells by using an emulsion transfer method originally developed by Pautot *et al.*<sup>21</sup> with modification. (Fig. 1B). The S48I48 was dissolved in an oil mixture of mineral oil:silicone oil (1:4) and a trace amount of fluorescent lipid, NBD-DPPE, was used to label peptide vesicles. Giant S48I48 vesicles recovered from the water phase had a range of sizes from 3 to > 50 μm with an average size of 15.1 μm

<sup>a</sup> Department of Mechanical Engineering, University of Michigan, Ann Arbor, Michigan 48109, USA

<sup>b</sup> Pritzker School of Molecular Engineering, University of Chicago, Chicago, Illinois 60637, USA

<sup>c</sup> Department of Biomedical Engineering, University of Michigan, Ann Arbor, Michigan 48109, USA

<sup>d</sup> Department of Chemical Engineering, University of Michigan, Ann Arbor, MI 48109, USA

<sup>e</sup> Cellular and Molecular Biology Program, University of Michigan, Ann Arbor, Michigan 48105, USA

<sup>f</sup> Department of Biophysics, University of Michigan, Ann Arbor, Michigan 48105, USA

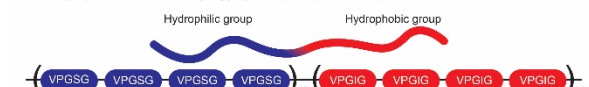
E-mail: Allen P Liu, [allenliu@umich.edu](mailto:allenliu@umich.edu)

Electronic Supplementary Information (ESI) available: [details of any supplementary information available should be included here]. See DOI: 10.1039/x0xx00000x

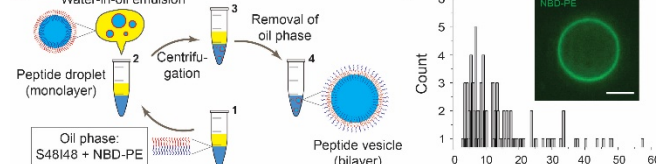
**(Fig. 1C).** To rule out the possibility that NBD-DPPE was somehow driving the formation of giant peptide vesicles, we made unlabeled S48I48 vesicles and incubated them with a cell membrane labelling dye, Vybrant DiO. We observed robust labeling of S48I48 vesicles (**Fig. 1D**). A control experiment with the same amount of NBD-DPPE used without including S48I48, no vesicles were formed (data not shown). We also tested the formation of peptide bilayer on a solid support (i.e., silica beads) using cell-free expressed ELP (**Methods, Fig. S2, ESI**). Together, these results demonstrate that amphiphilic ELPs can robustly form peptide vesicles and are compatible with emulsion transfer techniques.

To characterize these peptide vesicles, we first used AFM nanoindentation and determined the Young's modulus of ELP vesicles. A force vs distance curve was plotted showing the AFM tip approaching a vesicle, force application, and deflection in cantilever, as shown in **Fig. 2A**. Using the Maugis model to fit the data (**Fig. S3**), the average Young's modulus of ELP vesicle was found to be 455 Pa. We next conducted coarse-grained molecular dynamics simulations of the bilayer to predict its thickness and internal molecular structure. We present in **Fig. 2C** a snapshot of the fully relaxed bilayer at 300 K and 1 bar together with the partial density profiles for the  $(VPGSG)_{48}$  and  $(VPGIG)_{48}$  segments and water across the bilayer. We observed the bilayer to quickly adopt a well-defined structure and morphology that remained stable over the course of the 1.8  $\mu$ s production run, indicating that, consistent with experimental observations, and a stable bilayer configuration. The upper  $\sim 2.5$  nm of each leaflet of the bilayer defines a transition region within which we observe limited incursion of water into the bilayer. It should be noted that some previous studies on ELP coacervates suggest relatively high water amount inside the coacervates<sup>22,23</sup> while our simulation of the bilayer shows very limited water penetration. Experiments done by Frank *et al.*<sup>24</sup> also suggest fast water influx into ELP vesicles. It is thus possible

**A Amphiphilic elastin-like polypeptide (ELP) (S48I48)**



**B**



**D**

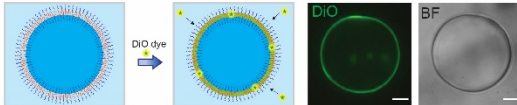


**Fig. 1 Generation of giant peptide vesicles.** (A) Amphiphilic ELP with 48 repeats of serine and isoleucine blocks constitute hydrophilic and hydrophobic domains, respectively. (B) Schematic representation of emulsion transfer method for giant peptide vesicles formation using ELP S48I48 with NBD-PE dye. (C) Peptide vesicle size distribution with average size 15.1  $\mu$ m; inset image of a single peptide vesicle labelled with NBD-PE.  $N_{\text{vesicles}} = 112$ . (D) Schematic illustration of peptide vesicle labelling with Vybrant DiO dye, representative brightfield and fluorescence images of a labelled S48I48 peptide vesicle at least after 1-hour labelling.

that, due to the large system size, we do not see water penetration in the time scale of our simulation and water penetration could happen in longer time scale. Our calculations predict the thickness of the each of the two distal hydrophilic S48 regions to be  $31.7 \pm 0.1$  nm, the central hydrophobic I48 region to be  $67.9 \pm 0.1$  nm, and the transition region between S48 and I48 regions to be  $3.0 \pm 0.1$  nm, for a total bilayer thickness of  $134.4 \pm 0.1$  nm.

Next, we sought to test how tough these peptide vesicles are against chemical and physical stresses. Triton-X 100 is well known for lipid membrane solubilization with a critical micelle concentration of  $\sim 0.02\%$  (w/v). As shown in **Fig. 2D**, almost 50% of peptide vesicles were stable against 0.3% of Triton-X 100 while lipid vesicles were completely disrupted at 0.04% of Triton-X 100. To assess ELP vesicles' physical stability, we challenge them with osmotic stress. In a hypo-osmotic condition, lipid vesicles were inflated and burst when an osmolarity difference of 193 mOsm (**Fig. 2E**) was reached. In contrast, peptide vesicles were stable even at the osmolarity difference of 507 mOsm (**Fig. 2E**).

Armed with a robust strategy to generate giant peptide vesicles, we next examined the capacity of these peptide vesicles for encapsulation of small molecules and proteins. As

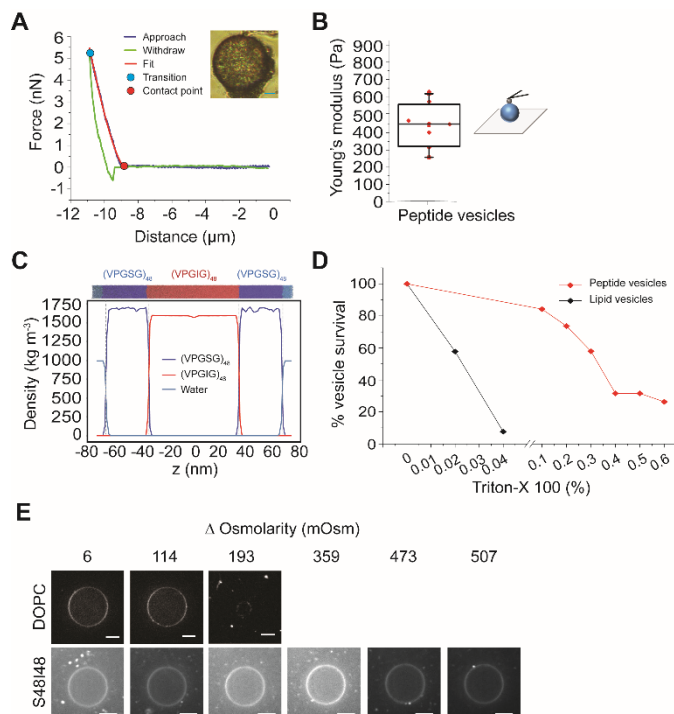


**Fig. 2 Characterisation of ELP vesicles.** (A) Force-displacement graph from AFM nanoindentation of peptide vesicles (insert) showing both approach and withdrawal curves. Scale bar 10  $\mu$ m. (B) Young's moduli calculated from single point AFM nanoindentation measurements of 8 peptide vesicles. (C) The terminal snapshot from a coarse-grained molecular dynamics simulation of the S48I48 bilayer together with the  $(VPGSG)_{48}$  and  $(VPGIG)_{48}$  segments and water partial density profiles calculated across the bilayer. The bilayer thickness is predicted to be  $(134.4 \pm 0.1)$  nm. (D) Stability of lipid and peptide vesicles against increasing concentrations of Triton-X 100. N-lipid vesicles and N-peptide vesicles analyzed were 26 and 19, respectively. (E) Representative images of lipid and peptide vesicles under hypo-osmotic shock,  $\Delta$  is the difference in osmolarity between inner and outer solutions. Scale bar 10  $\mu$ m.

expected from an emulsion transfer method, encapsulation of a small molecule dye (e.g., Rhodamine-B) was robust in S48I48 vesicles (Fig. 3A), and observable leakage of the encapsulated dye was not detected from overnight incubation at room temperature (RT) (data not shown).

We next examined the compatibility of bacterial CFE reactions with our newly developed peptide vesicle system and tested two scenarios: i) encapsulation of proteins expressed by a CFE reaction, and ii) encapsulation of a CFE reaction leading to *in situ* expression of proteins. Using GFP as a reporter, our home-made *E. coli* CFE robustly produced GFP over 4 hours (Fig. 3B). Expressed GFP was encapsulated and as expected, it was detected in S48I48 vesicles (Fig. 3C). Similarly, cell-free expression of GFP was detected in S48I48 peptide vesicles *in situ*, when CFE components were directly encapsulated and incubated (Fig. 3D). We did not observe any peptide membrane instability (resulted from growth or shrinkage) from the CFE reaction. These results demonstrate that giant S48I48 ELP peptide vesicles can host CFE reactions similar to giant lipid bilayer vesicles.

The growth of the vesicle, considered to be an important feature of synthetic cell development, can be achieved by the addition of membrane components<sup>25,26</sup> or by using lipid modifying enzymes either introduced as a purified protein<sup>27</sup> or by cell-free expression<sup>28</sup>. For ELP vesicles, a recent study reported by Frank *et al.*<sup>24</sup> showed the growth of peptide vesicles by a combination of Triton-X 100 (0.1%), osmotic imbalance, and extra ELP fed from the outside while hosting CFE reactions. Here we sought to directly incorporate cell-free expressed ELP into pre-formed ELP vesicles. For this purpose, we selected another ELP termed RQ-F: an amphiphilic ELP with sequence [(VPGRG)<sub>5</sub>(VPGQG)<sub>5</sub>]<sub>2</sub>(VPGFG)<sub>20</sub> with arginine (R) and glutamine (Q) blocks. The free lysine at position 30 (Table S1, ESI) can be fluorescently labelled *in situ* by FluoroTect Green Lys in the CFE reaction. We hypothesized that Green Lys labeled RQ-F (RQ-

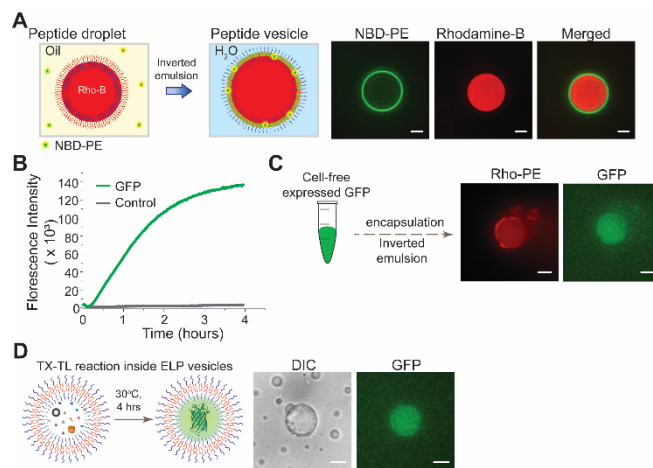


Fig. 3 Peptide vesicles as a chassis for synthetic cell. (A) Encapsulation of small molecules like rhodamine dye in a S48I48 vesicle. (B) Bulk expression of GFP by an *E. coli* CFE reaction incubated for 4 hours at 30°C. (C) Cell-free expressed protein (GFP) encapsulated inside peptide vesicles generated by emulsion transfer method and fluorescence images of GFP encapsulated in a S48I48 vesicle. (D) Schematic illustrating encapsulation of CFE reaction to express GFP. Brightfield and fluorescence images of S48I48 vesicle after 4 hours of expression at 30°C. Scale bars are 10  $\mu$ m.

F<sup>GreenLys</sup>) can be incorporated into a pre-existing ELP vesicle membrane (Fig. 4A). Cell-free expression of RQ-F<sup>GreenLys</sup> was confirmed by in-gel imaging as shown in Fig. 4B. When cell-free expressed RQ-F<sup>GreenLys</sup> was incubated (without purification) with S48I48 peptide vesicles under iso-osmotic conditions at RT for 3 hours, we observed clear uniform membrane incorporation of RQ-F<sup>GreenLys</sup> (Fig. 4C). The change in size of peptide vesicles due to membrane insertion was not significant enough to be detected by fluorescence microscopy. In distinct contrast, we did not find labeling of the membrane with only Green Lys alone in CFE reactions without expressing RQ-F.

Using an emulsion transfer method, we report micron-scale peptide vesicles made of amphiphilic S48I48 ELP. ELPs represent a desirable chassis material for synthetic cell construction for several reasons, including: (i) their stability in harsh physical and chemical conditions; (ii) inexpensive and relative ease of synthesis; (iii) ease of purification with high yield; (iv) and the ability to modify their polarity by introducing different guest residues. Unlike lipid vesicles, the S48I48 peptide vesicles appear to have a thick membrane, likely due to its large hydrophobic and hydrophilic blocks each constituting 240 amino acids. To our knowledge, peptide vesicles comprised of S48I48 reported here are the largest polypeptide sequence reported to form giant peptide compartments.

The first demonstration of using an amphiphilic ELP to create vesicular structures as reaction compartments for synthetic cells utilized a glass bead swelling method that yielded peptide vesicles ~200 nm in diameter.<sup>15</sup> Subsequently, the same group devised a solvent evaporation method using tetrahydrofuran (THF) to create ELP vesicles with two different sizes, ones that were tens of nanometer in diameter and others over 1  $\mu$ m in size.<sup>24</sup> Since the emulsion transfer method is commonly used for lipid vesicle encapsulation, its direct applicability to make peptide vesicles eliminates the use of harsh organic solvents like THF. Since the size of emulsion droplets can be controlled by using microfluidics, an emulsion

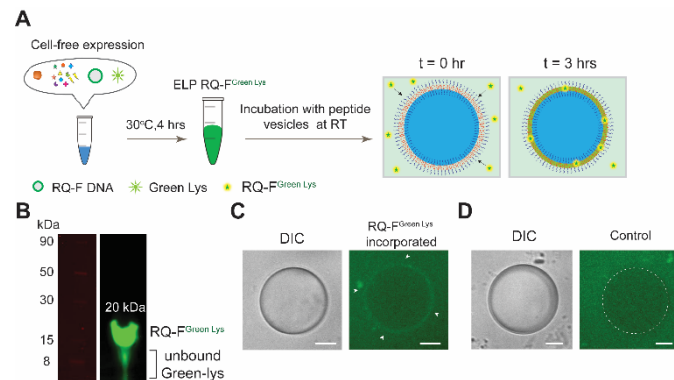


Fig. 4 Incorporation of ELP RQ-F<sup>GreenLys</sup> into the peptide membrane. (A) Schematic illustration of fluorescent labelling of ELP RQ-F by incorporating green lysine during CFE with FluoroTect Green Lys. Labelled RQ-F was added to the outer solution of the peptide vesicles and incubated for at least 3 hours at RT. (B) SDS-PAGE of the fluorescently labelled RQ-F with a trail of unreacted reagent. (C) Brightfield and fluorescence images of the ELP S48I48 peptide vesicle with RQ-F<sup>GreenLys</sup> inserted into the bilayer membrane. (D) Brightfield and fluorescence images of the ELP S48I48 peptide vesicle incubated with CFE reaction with green lysine but without RQ-F DNA. Scale bars are 10  $\mu$ m.

transfer method described here would allow for creation of peptide-based synthetic cells with homogeneous sizes. As with other emulsion-based methods for vesicle generation, we cannot rule out the possibility that there remains residual oil within the ELP bilayer.

Since the ELP vesicles were cell-sized, our AFM measurements yielded Young's modulus of peptide vesicles. Interestingly, the stiffness of ELP vesicles is comparable to whole cell stiffness.<sup>29,30</sup> Given that the stiffness of lipid and polymer membranes is highly dependent on membrane thickness,<sup>31</sup> we expect the membrane stiffness of ELP membranes is higher than lipid membranes (typically  $\sim 20$   $k_B T$ ).

In summary, this study presents an emulsion transfer method as a facile approach for generating giant peptide vesicles as a chassis material for synthetic cell research. We show the peptide vesicles membrane can be labeled with fluorescently labeled lipids or membrane dye. These giant peptide vesicles can host bacterial CFE reactions and express proteins of interest. We further demonstrate that ELPs expressed by CFE can incorporate into existing an ELP membrane. These highly stable peptide vesicles could serve as a robust platform to advance research in bottom-up synthetic biology.

S48I48 ELP was a kind gift from Andrew MacKay, University of Southern California, USA (Addgene plasmid no. 68394), RQ-F ELP was a kind gift from Tobias Pirzer, Technical University Munich, Germany. We thank Nicholas Stephanopoulos and Julio Bernal-Chanchavac (Arizona State University) for synthesizing and providing cholesterol-PEG-peptide K. This work is supported by the National Science Foundation under Grant Nos. DMR-1939354 (APL) and DMR-1939463 (ALF).

B.S., A.L.F., A.P.L conceived the study. B.S., A.P.L designed the experiments. B.S. performed the experiments. Y.M., A.L.F designed the simulation study, Y.M. carried out the simulation. H.H., B.M.B. designed the AFM characterization experiment, H.H. performed the AFM experiments. B.S., A.P.L wrote the paper. All authors contributed to the manuscript revision and approved the final version.

## Conflicts of interest

ALF is a co-founder and consultant of Evozyne, LLC and a co-author of US Provisional Patents 62/853,919 and 62/900,420 and International Patent Applications PCT/US2020/035206 and PCT/US20/50466.

## Notes and references

1. J. W. Szostak, D. P. Bartel and P. L. Luisi, *Nature*, 2001, **409**, 387–390.
2. P. Stano, *Life*, 2019, **9**, 3.
3. V. Noireaux and A. Libchaber, *Proc. Natl. Acad. Sci. U. S. A.*, 2004, **101**, 17669–17674.
4. S. Majumder, J. Garamella, Y. L. Wang, M. Denies, V. Noireaux

and A. P. Liu, *Chem. Commun.*, 2017, **53**, 7349–7352.

5. I. A. Chen, R. W. Roberts and J. W. Szostak, *Science (80-.)*, 2004, **305**, 1474–1476.
6. C. Martino, S.-H. Kim, L. Horsfall, A. Abbaspourrad, S. J. Rosser, J. Cooper and D. A. Weitz, *Angew. Chemie*, 2012, **124**, 6522–6526.
7. F. Caschera, J. W. Lee, K. K. Y. Ho, A. P. Liu and M. C. Jewett, *Chem. Commun.*, 2016, **52**, 5467–5469.
8. K. K. Y. Ho, J. W. Lee, G. Durand, S. Majumder and A. P. Liu, *PLoS One*, 2017, **12**, e0174689.
9. X. Huang, M. Li, D. C. Green, D. S. Williams, A. J. Patil and S. Mann, *Nat. Commun.*, 2013, **4**, 1–9.
10. M. L. Jacobs, M. A. Boyd and N. P. Kamat, *Proc. Natl. Acad. Sci.*, 2019, **116**, 4031–4036.
11. L. Sercombe, T. Veerati, F. Moheimani, S. Y. Wu, A. K. Sood and S. Hua, *Front. Pharmacol.*, 2015, **6**, 286.
12. B. M. Discher, Y. Y. Won, D. S. Ege, J. C. M. Lee, F. S. Bates, D. E. Discher and D. A. Hammer, *Science (80-.)*, 1999, **284**, 1143–1146.
13. E. Rideau, R. Dimova, P. Schwille, F. R. Wurm and K. Landfester, *Chem. Soc. Rev.*, 2018, **47**, 8572–8610.
14. A. Groaz, H. Moghimianaval, F. Tavella, T. W. Giessen, A. G. Vecchiarelli, Q. Yang and A. P. Liu, *WIREs Nanomedicine and Nanobiotechnology*, 2020, e1685.
15. K. Vogeley, T. Frank, L. Gasser, M. A. Goetzfried, M. W. Hackl, S. A. Sieber, F. C. Simmel and T. Pirzer, *Nat. Commun.*, 2018, **9**, 3862.
16. A. Schreiber, M. C. Huber and S. M. Schiller, *Langmuir*, 2019, **35**, 9593–9610.
17. D. W. Urry, *J. Phys. Chem. B*, 1997, **101**, 11007–11028.
18. D. E. Meyer and A. Chilkoti, *Nat. Biotechnol.*, 1999, **17**, 1112–1115.
19. M. K. Pastuszka, X. Wang, L. L. Lock, S. M. Janib, H. Cui, L. D. Delevé and J. A. MacKay, *J. Control. Release*, 2014, **191**, 15–23.
20. M. Shah, P. Y. Hsueh, G. Sun, H. Y. Chang, S. M. Janib and J. A. MacKay, *Protein Sci.*, 2012, **21**, 743–750.
21. S. Pautot, B. J. Frisken and D. A. Weitz, *Langmuir*, 2003, **19**, 2870–2879.
22. U. DW, T. TL and P. KU, *Biopolymers*, 1985, **24**, 2345–2356.
23. U. DW, H. T. S. M, G. HE, S. L, D. J, X. J and P. T, *Philos. Trans. R. Soc. Lond. B. Biol. Sci.*, 2002, **357**, 169–184.
24. T. Frank, K. Vogeley, A. Dupin, F. C. Simmel and T. Pirzer, *Chem. – A Eur. J.*, 2020, **26**, 17356–17360.
25. M. M. Hanczyc, S. M. Fujikawa and J. W. Szostak, *Science (80-.)*, 2003, **302**, 618–622.
26. T. F. Zhu and J. W. Szostak, *J. Am. Chem. Soc.*, 2009, **131**, 5705–5713.
27. A. Bhattacharya, R. J. Brea, H. Niederholtmeyer and N. K. Devaraj, *Nat. Commun.*, 2019, **10**, 1–8.
28. D. Blanken, D. Foschepoth, A. C. Serrão and C. Danelon, *Nat. Commun.*, 2020, **11**, 4317.
29. L. LM and L. AP, *Lab Chip*, 2015, **15**, 264–273.
30. W. Xu, R. Mezencev, B. Kim, L. Wang, J. McDonald and T. Sulcik, *PLoS One*, 2012, **7**, e46609.
31. E. Rideau, R. Dimova, P. Schwille, F. R. Wurm and K. Landfester, *Chem. Soc. Rev.*, 2018, **47**, 8572–8610.